Science Bulletin 69 (2024) 2174–2178

Contents lists available at ScienceDirect

Science Bulletin

journal homepage: www.elsevier.com/locate/scib

Short Communication

Hierarchical defect-rich UiO-66 membrane towards superior flue gas and butane isomer separations

Yanwei Sun [a,c], Jiahui Yan [a], Jie Jiang [a], Mingming Wu [a], Ting Xia [a], Yi Liu [a,b,*]

[a] State Key Laboratory of Fine Chemicals, Frontiers Science Center for Smart Materials, School of Chemical Engineering, Dalian University of Technology, Dalian 116024, China
[b] Dalian Key Laboratory of Membrane Materials and Membrane Processes, Dalian University of Technology, Dalian 116024, China
[c] Department of Chemistry, Faculty of Arts and Sciences, Beijing Normal University, Zhuhai 519087, China

ARTICLE INFO

Article history:
Received 8 February 2024
Received in revised form 2 April 2024
Accepted 27 May 2024
Available online 31 May 2024

Membrane technology has achieved significant progress in recent decades, primarily due to its attributes of high separation efficiency, low energy consumption, compact footprint, and affordable capital costs [1]. Metal-organic framework (MOF), a class of highly porous crystalline materials with ordered porous topology and tunable chemical functionality, has demonstrated great potential as superb membrane candidate [2]. Nonetheless, the trade-off between permeability and selectivity still remains. Deposition of uniform MOF seed layers comprising ultrathin nanosheets (NSs) followed by controlled epitaxial growth represents an effective protocol for reducing MOF membrane thickness, and therefore, diffusion resistance in the membrane. Nevertheless, under most circumstances, facile preparation of monodispersed MOF NSs remains a challenging task.

Introduction of hierarchy into membrane represents an alternative approach to alleviate diffusion resistance of guest molecules, relying on equivalent reduction in diffusion path length [3,4]. For instance, Choi and co-workers [5] prepared hierarchical mobil-type five (MFI) zeolite membranes containing siliceous self-pillared pentasil (SPP) zeolite-induced extrinsic mesopores, resulting in concurrently increased *p*-/*o*-xylene selectivity and *p*-xylene permeance compared with bulk MFI zeolite membranes. Very recently, we synthesized hierarchical MFI zeolite membrane comprising (*h*0*h*)-oriented top selective layer and bottom hollow layer on porous α-Al_2O_3 substrate with superior *n*-/*i*-C_4H_{10} separation performance [6]. Nevertheless, deliberate manipulation of pore environment (e.g., pore size, adsorption properties, and defective sites) in hierarchical membranes, which has been proven to exert a profound influence on the separation performance, still remains challenging.

UiO-66, which comprises $Zr_6O_4(OH)_4$ cluster nodes connected by 1,4-benzodicarboxylic acid, is regarded as an excellent candidate for membrane applications in CO_2 capture from flue gas due to suitable pore aperture size (~6 Å) and high-affinity interplay between coordinatively unsaturated $Zr_6O_4(OH)_4$ cluster nodes and CO_2. It has been proven that missing-linker defects in UiO-66 framework could be deliberately tailored through reaction condition optimization. An increase in missing-linker number enabled more sufficient exposure of coordinatively unsaturated $Zr_6O_4(OH)_4$ cluster nodes, and therefore, higher CO_2/N_2 selectivity, resulting in superior CO_2/N_2 selectivity towards defect-rich UiO-66 membranes [7]. In contrast, defect engineering was found to exert limited influence on CO_2 permeability.

Aiming at transcending the trade-off between CO_2 permeability and CO_2/N_2 selectivity, in this study, we pioneered the preparation of hierarchical defect-rich UiO-66 membranes with synthetic protocol briefly depicted as follow: Initially, hollow-structured UiO-66 nanoparticles (designated as H-UiO-66 NPs) were obtained through wet-chemical etching of bulk UiO-66 crystals (Fig. 1a). Subsequently, hollow-structured UiO-66 seed layer was deposited on porous α-Al_2O_3 substrate by spin-coating. Finally, single-mode microwave heating was conducted to obtain hierarchical defect-rich UiO-66 membrane with superior CO_2/N_2 separation performance.

The first step involved the preparation of H-UiO-66 NPs. Previous studies indicated that post-chemical etching represented an effective strategy for dissolving the interiors of MOFs, creating hollow structures with no loss in structural integrity [8,9]. Herein, we explored the preparation of uniform H-UiO-66 NPs via precise anisotropic etching of octahedral-shaped bulk counterparts (denoted as B-UiO-66 NPs) in Na_2WO_4 solution. Initially, B-UiO-66 NPs with an average size of 700 nm were synthesized following well-documented procedure (Fig. S1 online). However, it was observed

* Corresponding author.
E-mail address: diligenliu@dlut.edu.cn (Y. Liu).

https://doi.org/10.1016/j.scib.2024.05.043

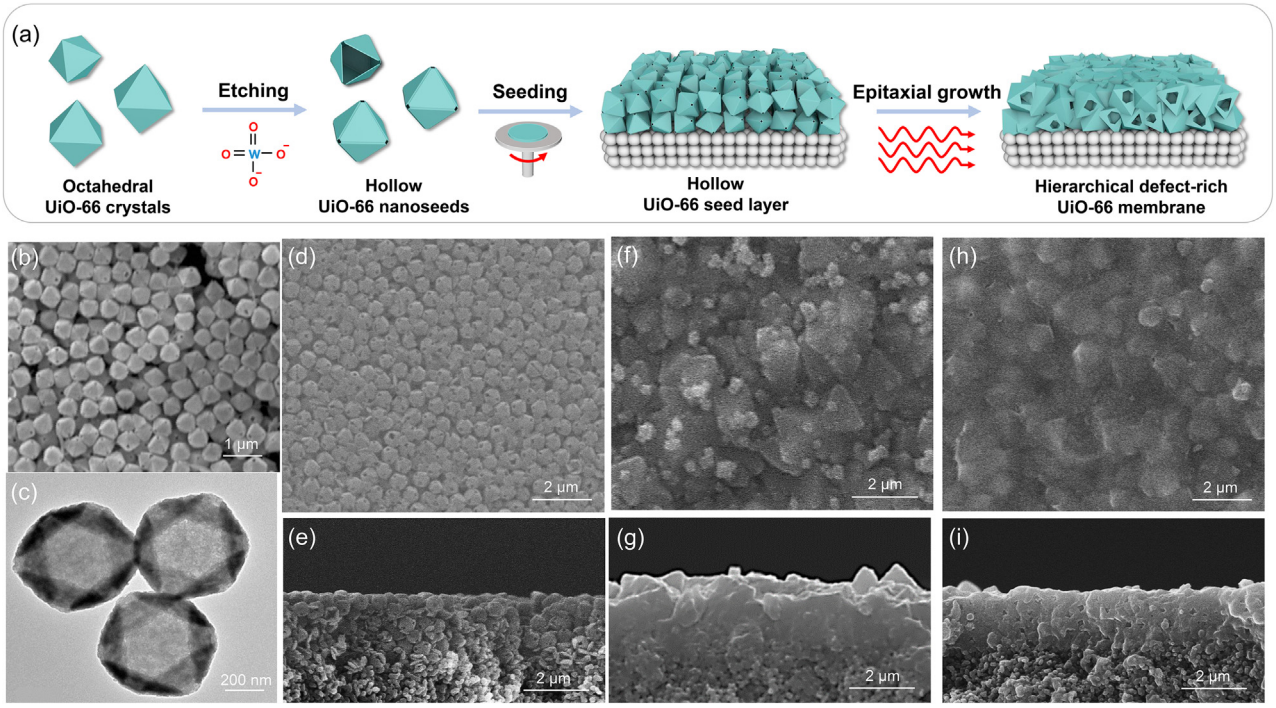

Fig. 1. Preparation and characterization of UiO-66 membranes. (a) Schematic illustration of the preparation of hierarchical defect-rich UiO-66 membrane. (b) Scanning electron microscope (SEM) and (c) transmission electron microscopy (TEM) image of hollow UiO-66 seeds. (d, e) SEM images of hollow UiO-66 seed layer. (f, g) SEM images of UiO-66 membrane prepared by conventional heating at 120 °C for 12 h, and (h, i) single-mode microwave heating at 100 °C for 30 min, respectively.

that conducting etching reaction under static heating condition led to non-uniform particle size distribution due to temperature and concentration gradients within reaction vessel (Fig. S2 online).

To obtain uniform H-UiO-66 NPs, a rotating convection oven was used instead to mitigate above gradients. As shown in Fig. 1b and c, after a reaction for 3 h, the interior of B-UiO-66 NPs had been largely dissolved, forming hollow-structured UiO-66 octahedrons with cavity size and shell thickness of ~600 and ~50 nm, respectively. Evidently, the etching process primarily targeted at interior regions of octahedral UiO-66 crystals, owing to their lower crystallinity in comparison with exterior facets, resulting in the formation of hollow-structured UiO-66 crystals. X-ray diffraction (XRD) patterns showed that H-UiO-66 NPs possessed the same characteristic peaks as B-UiO-66 NPs, signifying the preservation of framework integrity (Fig. S3 online). Furthermore, N_2 adsorption–desorption isotherms at 77 K of H-UiO-66 NPs featured a steep uptake at low relative pressure (P/P_0 = 0–0.02) and a hysteresis loop at P/P_0 = 0.45–1.0 (Fig. S4 online), indicating the presence of both mesopores and micropores on the shell of H-UiO-66 NPs. Through combining with hollow structure, we inferred that a hierarchically porous structure had been established. Notably, the BET surface area analysis revealed that the H-UiO-66 NPs possessed a surface area of 420 $m^2\ g^{-1}$, which was notably lower than that of B-UiO-66 NPs (1010 $m^2\ g^{-1}$) (Table S1 online). This discrepancy could be attributed to partial framework collapse. Structure deficiencies within the framework were subjected to further evaluation via potentiometric acid-base titration. Calculation results revealed an increase in missing-linker number from 1.6 to 1.7 after etching treatment (Fig. S5 and Table S2 online), which was beneficial for achieving higher CO_2/N_2 selectivity.

Spin-coating was conducted for depositing the seed layer. As shown in SEM images (Fig. 1d, e), after spin-coating, the substrate surface had been covered with uniform UiO-66 seed layer with a thickness of 2.1 μm, approximately equivalent to 3–4 single layers of H-UiO-66 NPs. It was worth mentioning that uniform dispersion of hollow-structured UiO-66 seeds in the suspension was crucial for obtaining uniform seed layers. To achieve this goal, thorough rinsing of H-UiO-66 NPs after etching was necessary; otherwise, agglomerated seeds would be sparsely dispersed on substrate surface (Fig. S6 online).

Subsequently, the process proceeded to epitaxial growth, which aimed to seal intergranular gaps present in the seed layer. Initially, solvothermal heating was utilized for this purpose. The experimental outcomes demonstrated that a well-intergrown UiO-66 membrane could be successfully fabricated under optimized conditions (Fig. 1f, Table S3 online). Nevertheless, internal cavities of UiO-66 seeds had been completely filled, resulting in the loss of hierarchical structure (Fig. 1g). To preserve internal cavities inherited from UiO-66 seeds, conducting epitaxial growth under milder reaction conditions had become indispensable. It has been proven that utilizing single-mode microwave heating during the epitaxial growth enabled not only significant reduction in reaction duration but also milder reaction condition with no compromise in membrane continuity, relying on its unique non-thermal effect [10,11]. Indeed, our results indicated that well-intergrown UiO-66 membrane could be obtained at 100 °C within 30 min under single-mode microwave heating (Fig. 1h). Cross-sectional SEM image (Fig. 1i) showed that obtained UiO-66 membrane (denoted as H-UiO-66) consisted of 190 nm-thick top layer and 220 nm-sized porous bottom layer, implying that the hollow structure in H-UiO-66 seeds had been largely preserved during epitaxial growth. The hierarchical porous structure was further confirmed by the analysis of N_2 sorption isotherms (Fig. S7 online), giving comprehensive combination of Type-I(a), Type-II and Type-IV(a) isotherms, which were characteristics of micropores, macropores, and mesopores, respectively, according to the International Union of Pure and Applied Chemistry (IUPAC) classification. This could be attributed to rapid formation of continuous top layer, functioning as a diffusion barrier. This barrier effectively hindered further

interaction between seed layer and bulk solution, thereby preserving the hollow structure. Furthermore, the generality of this approach was further verified by the successful preparation of hierarchical NH_2-UiO-66 membrane (Fig. S8 online).

It is noteworthy that UiO-66 seed morphology exerted significant influence on the structure of UiO-66 membranes. For comparison, a UiO-66 membrane was further prepared using B-UiO-66 NPs as seeds while keeping other synthetic conditions unchanged. After epitaxial growth, well-intergrown UiO-66 membrane with a thickness of 2.4 μm was successfully obtained (Fig. S9 online). Phase purity of the membrane could be convinced by the XRD pattern (Fig. S10 online). Of particular note, the ratio of peak intensity between (111) and (002) planes was calculated to be 8.29, which was higher than that of B-UiO-66 membrane (5.18), revealing a higher degree of (111)-preferred orientation for H-UiO-66 membrane. This could be attributed to increased proportion of (111) facets in H-UiO-66 NPs due to selective etching of octahedrons, which led to preferred (111)-oriented seed layer (Fig. S11 online), thereby promoting preferential epitaxial growth of (111) facets. Moreover, as mentioned in previous reports, adopting such preferred orientation enabled a significant reduction in grain boundary defects and diffusion path length, which was quite beneficial for enhancing separation efficiency.

To investigate the effect of heating mode on framework structure, UiO-66 powders deposited at the bottom of the vessel after conventional heating (denoted as C-UiO-66) and single-mode microwave heating (denoted as SM-UiO-66) were collected and characterized. As depicted in Fig. S12 (online), the size of SM-UiO-66 crystals reached 260 nm, a notably smaller dimension when compared to those synthesized using conventional heating methods (~1 μm), which could be attributed to the rapid and volumetric dielectric heating under microwave irradiation. Both XRD patterns and Fourier transform infrared spectroscopy (FT-IR) spectra, as shown in Fig. S13 (online), respectively, were consistent with the standard UiO-66 phase. This affirmation confirms that the alteration in heating mode did not impact their phase purity or functionality. Recognizing the significance of the pore environment in separation efficiency, thermogravimetric (TG) analysis was subsequently conducted to quantify the deficiencies in linkers within UiO-66 powders (Fig. S14 online). Employing the methodology developed by Lillerud and co-workers [12], the missing-linker count per $Zr_6O_4(OH)_4$ node within the SM-UiO-66 framework was calculated to be 2.5, which is substantially higher than that of C-UiO-66 (1.4). Higher defect density in SM-UiO-66 framework could also be confirmed by reduced acetate/BDC ratio in dissolution/^{1}H nuclear magnetic resonance (NMR) spectra (Fig. S15 online). The above results convincingly demonstrated that conducting epitaxial growth under single-mode microwave heating led to a significant increase in the number of missing linkers, which could be attributed to the accelerated crystal growth kinetics under microwave heating [13].

Simultaneously, textural properties of obtained UiO-66 powders were examined using N_2 adsorption–desorption isomers (77 K). All samples showed typical type I isotherms, confirming the presence of microporous structure (Fig. S16 online). In addition, CO_2 adsorption capacity (69.3 $cm^3\ g^{-1}$) of SM-UiO-66 was higher than that of C-UiO-66 (60.9 $cm^3\ g^{-1}$), implying that CO_2 was preferentially adsorbed on SM-UiO-66 with higher missing-linker number (Fig. S17 online). Furthermore, equimolar CO_2/N_2 IAST selectivity (298 K) was calculated considering its positive correlation with membrane selectivity. Our results indicated that the CO_2/N_2 IAST selectivity of SM-UiO-66 and C-UiO-66 was 37.4 and 27.3, respectively (Table S4 online), implying that employing single-mode microwave heating was beneficial for enhancing the CO_2/N_2 selectivity of UiO-66 membranes.

Finally, gas permeation test was conducted to evaluate the CO_2/N_2 separation performance of obtained UiO-66 membranes. As depicted in Fig. 2a, the CO_2 permeance was much higher than other gas molecules. CO_2/N_2 separation factor of H-UiO-66 membrane reached 37.1 with CO_2 permeance of 2113 gas permeance unit (GPU), which were 2.1 and 16.2 times higher than C-UiO-66 membrane (Fig. 2b, and Table S5 online). In particular, its CO_2/N_2 separation performance not only well surpassed state-of-the-art UiO-66 membranes but also transcended majority of pure MOF membranes (Table S6 online). Remarkedly enhanced separation performance could be attributed to the presence of hierarchical structure on a mesoscopic scale and higher missing-linker number on a microscopic scale, which led to reduced diffusion path length (i.e., higher CO_2 permeance) and more CO_2 adsorption sites (i.e., higher CO_2/N_2 selectivity), as illustrated in Fig. 2d. Considering its practical application, the CO_2/N_2 separation performance on H-UiO-66 membrane in the presence of water vapor was further investigated (Table S7 online). Gas permeation results demonstrated that its CO_2/N_2 separation performance still met industry requirements, i.e., CO_2/N_2 selectivity and CO_2 permeance higher than 30 and 1000 GPU respectively.

To gain insights in gas diffusion mechanism of UiO-66 membranes, their gas permeance was deconvoluted into sorption and diffusion coefficients as described in Table S8 (online). Their sorption coefficients, diffusion coefficients, sorption selectivity, and diffusion selectivity were calculated and shown in Fig. 2c, e. As expected, H-UiO-66 membrane showed higher diffusivity and sorption coefficients for CO_2 than those of C-UiO-66 and B-UiO-66 membranes. Correspondingly, the CO_2/N_2 diffusivity selectivity (2.94) and solubility selectivity (12.37) of H-UiO-66 membrane were higher. Therefore, superior CO_2/N_2 separation performance could be interpreted by preferential diffusion and adsorption for CO_2 relative to N_2 in the membrane.

In addition to flue gas separation, UiO-66 holds great potential for separating n-C_4H_{10} from i-C_4H_{10} based on their discrepancy in configuration. It has been demonstrated that the diffusivity of n-C_4H_{10} within UiO-66 framework was notably higher compared with that of i-C_4H_{10} as supported by both experimental ^{2}H NMR and molecular dynamics (MD) simulation results [14]. Much higher diffusivity originated from elongated shape of n-C_4H_{10} molecules, allowing them to freely shift between tetrahedral cages in the UiO-66 framework. Herein the n-/i-C_4H_{10} separation performance of H-UiO-66 membrane was investigated further. For the single gas, its ideal n-/i-C_4H_{10} selectivity reached 22.5 with n-C_4H_{10} permeance of 552 GPU (Fig. 2f and Table S9 online), implying that n-C_4H_{10} with purity higher than 95% could be obtained through a single-stage membrane process, fulfilling the prerequisites for n-C_4H_{10} isomerization and ethylene cracking. Moreover, in comparison with previous literature, H-UiO-66 membrane demonstrated near 10-fold increase in n-C_4H_{10} permeance (Fig. 2g and Table S10 online), which was quite beneficial for enhancing its separation efficiency. Furthermore, we noticed that the separation factor for n-/i-C_4H_{10} mixture was slightly reduced relative to its ideal selectivity, which could be ascribed to competitive adsorptions of n-C_4H_{10} and i-C_4H_{10} in the framework, as convinced by gas sorption isotherms (Fig. S18 online).

To determine the origin of the n-/i-C_4H_{10} selectivity of prepared H-UiO-66 membrane, n-/i-C_4H_{10} separation performance of C-UiO-66 membrane was further investigated. Correspondingly, sorption selectivity and diffusion selectivity of obtained membranes were further calculated according to gas sorption isotherms and membrane permeability. As shown in Fig. S18 (online), n-C_4H_{10} adsorption capacity (103.1 $cm^3\ g^{-1}$) of SM-UiO-66 was higher than that of C-UiO-66 (63.2 $cm^3\ g^{-1}$), implying that n-C_4H_{10} was preferentially adsorbed on SM-UiO-66 with higher missing-linker number,

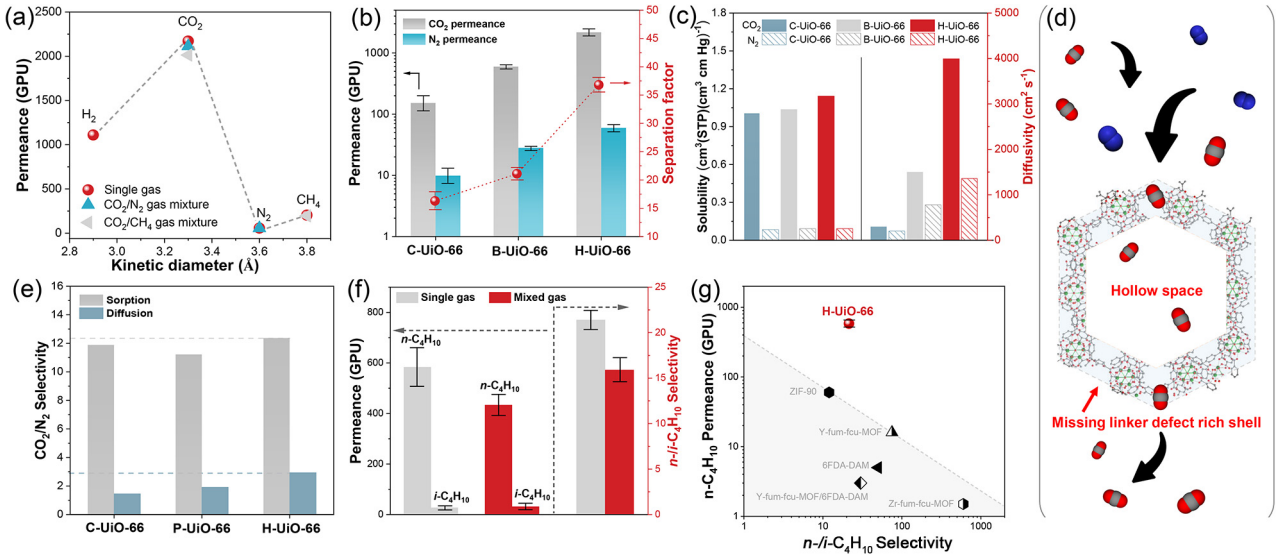

Fig. 2. Separation performance for UiO-66 membranes. (a) Single and mixed gas permeances of H-UiO-66 membrane measured under ambient conditions. (b) Comparison of the CO_2/N_2 separation performance of UiO-66 membranes. (c) Gas solubility and diffusivity of UiO-66 membranes. (d) Gas diffusion in hollow-structured UiO-66 crystal with missing-linker defects. (e) CO_2/N_2 sorption and diffusion selectivity of UiO-66 membranes. (f) *n*-/*i*-C_4H_{10} separation performance of H-UiO-66 membrane. (g) Comparison of the *n*-/*i*-C_4H_{10} separation performance of H-UiO-66 with reported MOF based membranes. Permeance and selectivity values are averaged over three membranes, and error bars correspond to the standard deviation.

resulting in higher solubility selectivity (Table S11 online). Simultaneously, H-UiO-66 membrane exhibited high *n*-/*i*-C_4H_{10} diffusion selectivity of 18.8, which could be ascribed to inherent configuration discrepancy of butane isomers. Notably, *n*-C_4H_{10} and *i*-C_4H_{10} took on linear and spherical-like configuration, respectively, with noticeable discrepancy in cross-sectional kinetic diameters [15]. Therefore, superior *n*-/*i*-C_4H_{10} separation performance can be attributed to the preferential diffusion and adsorption of *n*-C_4H_{10} in the membrane.

Finally, to verify the reproducibility of this synthetic protocol, two additional H-UiO-66 membranes were prepared and employed in CO_2/N_2 and *n*-/*i*-C_4H_{10} separation. Gas permeation results indicated that all of them exhibited excellent separation performances with small standard deviation (Tables S5 and S9 online), thereby demonstrating that this synthetic protocol was reliable in terms of reproducibility.

To summarize, in this study hierarchical defect-rich UiO-66 membranes featuring ultrathin oriented selective top layer, hollow-structured bottom layer, and high missing-linker number in the framework were prepared by combining hollow-structured UiO-66 seeds with single-mode microwave heating-assisted epitaxial growth. High uniformity and intensity of single-mode microwave heating expedited formation of hierarchical and defective membrane structure, ultimately leading to superior CO_2/N_2 separation performance. Moreover, the multi-scale structure superiority conferred upon UiO-66 membranes enabled them to achieve *n*-/*i*-C_4H_{10} separation performance surpassing state-of-the-art pristine pure MOF membranes, suggesting its great potential for enhancing the separation performance of various MOF membranes.

Conflict of interest

The authors declare that they have no conflict of interest.

Acknowledgments

This work was supported by the National Natural Science Foundation of China (22108025 and 22078039), the Science Fund for Creative Research Groups of the National Natural Science Foundation of China (22021005), the National Key R&D Program of China (2023YFB3810700), and the Fundamental Research Funds for the Central Universities (DUT22LAB602).

Author contributions

Yi Liu conceived the research idea. Yi Liu and Yanwei Sun designed the experiments. Yanwei Sun performed major experiments and analyzed the experimental data. Jiahui Yan helped with the calculation of gas separation IAST. Jie Jiang helped with the synthesis of UiO-66 crystals. Mingming Wu and Ting Xia helped with the SEM images. Yi Liu and Yanwei Sun wrote the paper with contributions from all authors.

Appendix A. Supplementary materials

Supplementary materials to this short communication can be found online at https://doi.org/10.1016/j.scib.2024.05.043.

References

[1] Sholl DS, Lively RP. Seven chemical separations to change the world. Nature 2016;532:435–7.
[2] Denny MS, Moreton JC, Benz L, et al. Metal–organic frameworks for membrane-based separations. Nat Rev Mater 2016;1:16078.
[3] Caro J. Hierarchy in inorganic membranes. Chem Soc Rev 2016;45:3468–78.
[4] Snyder MA, Tsapatsis M. Hierarchical nanomanufacturing: From shaped zeolite nanoparticles to high-performance separation membranes. Angew Chem Int Ed 2007;46:7560–73.
[5] Hong S, Jeong Y, Baik H, et al. An extrinsic-pore-containing molecular sieve film: A robust, high-throughput membrane filter. Angew Chem Int Ed 2021;60:1323–31.
[6] Liu Y, Li M, Chen Z, et al. Hierarchy control of MFI zeolite membrane towards superior butane isomer separation performance. Angew Chem Int Ed 2021;60:7659–63.
[7] Yan J, Ji T, Sun Y, et al. Room temperature fabrication of oriented Zr-MOF membrane with superior gas selectivity with zirconium-oxo cluster source. J Membr Sci 2022;661:120959.
[8] Cai ZX, Wang ZL, Xia YJ, et al. Tailored catalytic nanoframes from metal-organic frameworks by anisotropic surface modification and etching for the hydrogen evolution reaction. Angew Chem Int Ed 2021;133:4797–805.
[9] Wei J, Cheng N, Liang Z, et al. Heterometallic metal-organic framework nanocages of high crystallinity: An elongated channel structure formed in situ through metal-ion (M = W or Mo) doping. J Mater Chem A 2018;6:23336–44.

[10] Sun Y, Hu S, Yan J, et al. Oriented ultrathin π-complexation MOF membrane for ethylene/ethane and flue gas separations. Angew Chem Int Ed 2023;62:e202311336.
[11] Sun Y, Song C, Guo X, et al. Microstructural optimization of NH_2-MIL-125 membranes with superior H_2/CO_2 separation performance by innovating metal sources and heating modes. J Membr Sci 2020;616:118615.
[12] Shearer GC, Chavan S, Ethiraj J, et al. Tuned to perfection: Ironing out the defects in metal-organic framework UiO-66. Chem Mater 2014;26:4068–71.
[13] Weeks JD, Gilmer GH. Dynamics of crystal growth. Adv Chem Phys 2007;40:157–228.
[14] Khudozhitkov AE, Arzumanov SS, Kolokolov DI, et al. UiO-66(Zr) MOF as a promising material for butane isomers separation: Evidence based on the analysis of the adsorbed alkanes mobility by 2H NMR and molecular dynamics simulation. J Phys Chem C 2021;125:13391–400.
[15] Zhou Y, Wang Y, Ban Y, et al. Carbon molecular sieving membranes for butane isomer separation. AICHE J 2019;65:e16749.

Yanwei Sun is currently an associate professor at Faculty of Arts and Sciences, Beijing Normal University. She majored in Chemical Processing at Dalian University of Technology under the supervision of Prof. Yi Liu and received her Ph.D. degree. Since 2021, she continued to work as a postdoctoral fellow at Dalian University of Technology. Her research interest mainly focuses on rational design and microstructure optimization of metal-organic framework (MOF) membranes/films, especially crystallographic oriented and ultrathin Ti/Zr-MOF based membranes for energy-efficient gas separation.

Yi Liu received his Ph.D. degree from Dalian Institute of Chemical Physics, Chinese Academy of Sciences in 2012. In 2012–2015, he worked as an Alexander von Humboldt research fellow at Leibniz Universität Hannover, Germany. In 2015–2016, he worked as a postdoctoral fellow at Kyoto University. He joined Dalian University of Technology as a professor in 2016. His research interest includes multi-scale optimization of zeolite, MOF, and low-dimensional membranes for potential use in gas separation, ion sieving, and water treatment.